



# Determination of Dielectric Function of Water in THz Region in Wood Cell Wall Result in an Accurate Prediction of Moisture Content

Han Wang<sup>1</sup> · Tetsuya Inagaki<sup>1</sup> · Ian D. Hartley<sup>2</sup> · Satoru Tsuchikawa<sup>1</sup> · Matthew Reid<sup>2</sup>

Received: 20 March 2019 / Accepted: 10 April 2019 / Published online: 27 April 2019

© Springer Science+Business Media, LLC, part of Springer Nature 2019

## Abstract

This report follows up previous work that presented a model for the simultaneous detection of moisture content and density of wood using Terahertz time-domain spectroscopy. A significant improvement in the prediction accuracy of the model is demonstrated by including a moisture content-dependent dielectric function for the water within the wood samples. Justification for using the dielectric function is presented, the prediction accuracy is quantified, and the results compared with prior work.

**Keywords** Terahertz time-domain spectroscopy · Wood · Density · Moisture content · Effective medium theory · Dielectric function

## 1 Introduction

Wood materials, which are the main product of the forestry industry, have many advantages over other building materials concerning strength, versatility, and sustainable design [1]. Physical properties of wood, such as density, moisture content (MC), and modulus of elasticity, have a substantial intrinsic variability within and between different species that significantly influence mechanical characteristics such as strength and stiffness [1]. It is therefore necessary for industrial production involving wood to measure these physical properties accurately in order to control product quality.

The main chemical components of the cell wall in wood are lignin and celluloses, which themselves have great potential as structural materials because of their high specific strength

---

✉ Tetsuya Inagaki  
inatetsu@agr.nagoya-u.ac.jp

<sup>1</sup> Graduate School of Bioagricultural Sciences, Nagoya University, Furo-cho Chikusa-ku, Nagoya 464-8601, Japan

<sup>2</sup> Department of Physics, University of Northern British Columbia, Prince George, BC V2N 4Z9, Canada

and large aspect ratio [2]. Since the components of the cell wall in different species of wood are similar, the density of the cell wall is approximately constant, exhibiting a value of close to  $1.4 \text{ g cm}^{-3}$  [3]. Therefore, the large observed variations in wood density are primarily related to the relative proportions of cell walls and lumens (air content), and the changing of moisture content, which is geometric in nature.

The behavior of water within the wood is not simple, and it changes with moisture content as a result of interaction within the cellulose matrix through hydrogen bonding, similar to the behavior of water with lipids, for example [4]. There is “free” water, which exists in wood as liquid water or water vapor in the lumen or free space (internal air voids), and “bound” water which interacts with electric fields very differently as it is subject to hydrogen bonding in the amorphous region on the surface crystallization region of cellulose, hemicellulose, and cellulose [5]. The fiber saturation point (FSP) is defined as the MC at the transition point from the saturated state to the unsaturated state, that is, where lumens have no liquid water [6], around a MC of 25–30%. The FSP defines an expected crossover from a “bound” water behavior to a “free” water behavior as additional water is introduced into the wood with increasing moisture content above the FSP.

Another aspect of moisture content in wood is related to its utility. In particular, dimensional change is a function of moisture content, which strongly affects physical and mechanical properties of wood [5]. During the processing of wood in the factory, the environmental humidity is the main factor affecting the MC of the wood. Wood absorbs and desorbs water periodically from the surrounding environment, which in turn leads to dimensional changes, and may even cause some cracking and warping [7]. Thus, detecting the density and MC of wood materials has important practical significance for evaluating their durability and service life.

Terahertz (THz) is electromagnetic radiation with frequencies in the range of 100–10 THz. New developments in technology to access this part of the electromagnetic spectrum are providing unique opportunities for technological innovation, national security, and economic development. THz technology has been shown to be a suitable tool for producing high-resolution images for wood, for example, in dendrochronology [8], and density mapping of wood [9]. There have already been some cases where THz technology has been applied in the wood industry. It has been demonstrated that THz can be used to identify wood species [10] and probe the water content distribution in wood materials [11].

Effective medium theory at THz frequencies has been applied to and used to successfully model heterogeneous dielectric mixtures [12] and to investigate water absorption in wood plastic composites [13]. Since wood can be considered a mixture of cell wall, air, and water, applying an effective medium theory to study wood is very suitable.

In previous work, it was demonstrated that THz time-domain spectroscopy (THz-TDS) can be used to detect density of oven-dry wood [14], as well as to simultaneously detect wood density and MC below the FSP with a relatively high degree of accuracy [15]. Simultaneous prediction of MC and density was made possibly by using a model that combined Bruggeman and Maxwell-Garnett effective medium theories (EMT's), and modeling the dielectric function of water using a double Debye model (as normally applied to bulk liquid water) with parameters taken from the literature [16]. However, the MC tends to be systematically underestimated in the prediction made using this model. The reason for the systematic inaccuracy is the assumption that the dielectric function of water within the wood is that of bulk, liquid water described by the Debye model. As discussed above, there is a transition from “bound” to “free” water with increasing moisture content, and therefore, not only is the

dielectric function of water within wood not that of bulk free water (at low moisture contents below the FSP), it is also strongly dependent on the MC. In the research reported here, the assumption of a constant, MC-independent dielectric function of water is removed; a species-independent calibration is performed to determine the MC-dependence of the dielectric function and used to optimize the simultaneous prediction of density and MC below the FSP. A significant improvement in the density and moisture content prediction accuracy is reported.

## 2 Material and Methods

### 2.1 Sample Preparation

As reported in our previous work [15], aspen (*Populus tremuloides*, oven-dry density of  $\rho_{\text{ovenwood}} \sim 0.49 \text{ g cm}^{-3}$ , hardwood), birch (*Betula spp.*,  $\rho_{\text{ovenwood}} \sim 0.64 \text{ g cm}^{-3}$ , hardwood), western hemlock (*Tsuga heterophylla*,  $\rho_{\text{ovenwood}} \sim 0.36 \text{ g cm}^{-3}$ , softwood), and maple (*Acer saccharum*,  $\rho_{\text{ovenwood}} \sim 0.72 \text{ g cm}^{-3}$ , hardwood) were obtained from a local supplier. Samples were cut from the radial plane with an approximate 5 mm (tangential direction) thickness and 30 mm (longitudinal direction)  $\times$  30 mm (radial direction) squares, the wood grain is parallel to the edge as shown in Fig. 1. For each species, three groups of five smooth, polished samples were prepared.

First, the samples were dried in a convection oven at  $103 \pm 2 \text{ }^\circ\text{C}$  for 48 h to determine the oven-dried mass and weighed ( $\pm 0.01 \text{ g}$ ) before and after the THz measurements to ensure that the samples did not absorb water from the atmosphere. The dimensions (length, width, and thickness) of all samples were measured using a caliper ( $\pm 0.01 \text{ mm}$ ) prior to THz measurement. After completing the THz measurement of the oven-dried wood, the samples were placed in a desiccator at different relative humidities (RH) to obtain different MC samples, and the RH was gradually controlled using a saturated salt solution. The salts used were anhydrous calcium sulfate ( $\text{CaSO}_4$ , RH = 0%), potassium hydroxide (KOH, RH = 8%), potassium fluoride (KF, RH = 30%), sodium chromate ( $\text{Na}_2\text{Cr}_2\text{O}_7 \cdot 2\text{H}_2\text{O}$ , RH = 54%), ammonium chloride ( $\text{NH}_4\text{Cl}$ , RH = 77%), and potassium nitrate ( $\text{KNO}_3$ , RH = 94%) obtained from SIGMA-

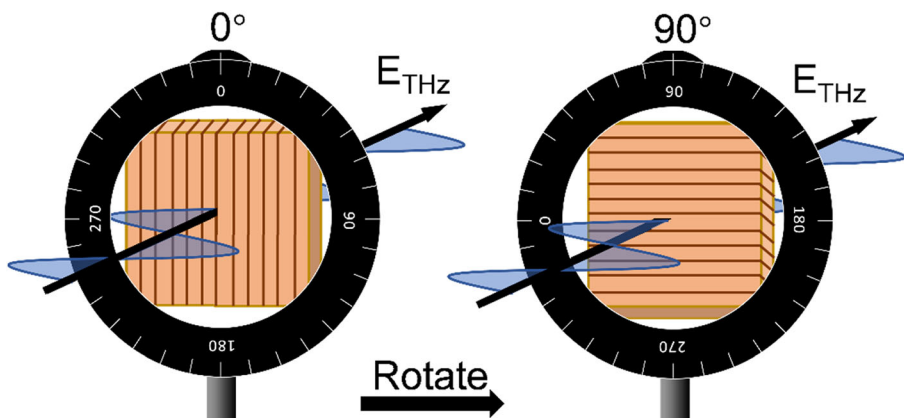


**Fig. 1** Polarization of the THz beam and the manual rotation stage to switch the directions of the sample. Zero degree and 90° are corresponding to polarizations perpendicular and parallel to the visible grain

ALDRICH. Ninety-nine percent RH was obtained using a desiccator with water only. The samples were placed in the desiccator for at least 48 h to ensure they reached an equilibrium MC. After equilibrium was reached, as determined by no change in mass, samples are taken out of the desiccators and their mass and dimensions are recorded. THz measurements were taken immediately for two THz field polarizations (parallel and vertical) relative to the visible grain of the wood; the THz measurements were very fast (10 s for each measurement). And the masses of the samples were also recorded after the THz measurement to ensure that the samples did not absorb or desorb water. Samples were measured oven-dry, followed by 11% RH, and progressively higher RH's. Densities and MC were calculated from physical dimensions, the average mass of the samples and the mass of the oven-dried wood samples. The above process was repeated for each sample from low to high MC. Experiments and wood conditioning were carried out at room temperature ( $21 \pm 1$  °C).

## 2.2 THz Spectral Measurement

Polarized THz transmission spectroscopy was performed using a modified Picometrix T-Ray 4000 THz spectrometer. This system produces THz measurements in an 80 ps window at a rate of 1000 waveforms per second. The bandwidth extends from approximately 0.01–2.00 THz. The emitter and detector are fiber-coupled photoconductive switches, generating linearly polarized THz radiation, where the polarization direction is defined by the orientation of the photoconductive antenna. The emitter and receiver photoconductive antennas are arranged with their linear polarization axis in the horizontal direction in the lab frame of reference. For each species of wood studied, the time-domain waveforms of the transmitted THz radiation were recorded at  $0^\circ$  and  $90^\circ$  orientations of the grain with respect to the THz polarization. Wood samples are mounted on a manual rotation stage with an accuracy of rotation of approximately  $\pm 0.25^\circ$ . When the sample was rotated to  $0^\circ/90^\circ$ , the grain of wood is perpendicular/parallel to the THz polarization as shown in Fig. 1. Each measurement has an average of 10,000 waveforms. A reference THz signal without a wood sample in place was obtained prior to each transmission measurement. The sample sizes were chosen to be larger than the THz beam diameter to avoid diffraction effects. The THz spectroscopy was performed in transmission, with a THz beam diameter ( $1/e$  electric field) of approximately 30 mm. The complex refractive index of the samples was determined from a transmitted and reference THz pulse according to Duvillaret et al.'s report [17] in the thick sample approximation as outlined in Reid et al.'s report [18]. The complex refractive index (with real and imaginary components) was used to calculate the dielectric function, which is the relevant parameter in applying the effective medium theories (EMTs) described in this work.

## 2.3 Model Construction

To predict density and MC from the measured THz spectra, a model that describes the dependence of the dielectric function on density and MC is required. The geometry of oven-dry wood can be considered being composed of cylinders of air in a background matrix consisting of the cell wall material. Using this concept, optical properties can be extracted from THz measurements using effective medium theory [14], based on the composite cylinder assemblage (CCA) formalism [19]. In this formalism, the effective medium properties are determined by inserting an infinite cylinder with dielectric function  $\epsilon_1$  into a concentric

cylindrical shell with dielectric function  $\varepsilon_2$ . This geometry has a unique axial direction and therefore depends on the polarization of the probing THz field.

For the case where the field is polarized perpendicular to the cylinder axis, an upper bound of the effective dielectric function in the CCA scheme is given by the Maxwell-Garnett (MG) formula:

$$\varepsilon_{\text{eff}}^{\perp, \text{max}} = \varepsilon_2 + \frac{f_1}{\frac{1}{\varepsilon_1 - \varepsilon_2} + \frac{f_2}{2\varepsilon_2}} \quad (1)$$

and when the field is polarized along the cylinder axis, where the electric field is always parallel to the dielectric interface, it follows the simple mixing rule [20]:

$$\varepsilon_{\text{eff}}^{\parallel} = f_1 \varepsilon_1 + f_2 \varepsilon_2 \quad (2)$$

where  $\varepsilon_1$  and  $f_1$  correspond to the dielectric function and the volume fraction of the infinite cylinder, with  $\varepsilon_2$  and  $f_2$  the dielectric function and the volume fraction of the cylindrical shell.

In the first step of applying this model, the dielectric function of the cell wall material is calculated from the measured values of the dielectric function of oven-dry wood samples. The result is averaged over the frequency range of 0.1–0.2 THz and over all samples measured. Subsequently, a single, frequency-independent value (the average outlined previously) is used in the model. This can be considered a calibration step, as further measurements to determine the dielectric properties of the cell wall are not required. The real and imaginary parts of the dielectric function are defined as  $\varepsilon' + i\varepsilon'' = (n + i\kappa)^2$ , the components of which are obtained from the measured refractive index and absorption coefficient. By using the MG-EMT model (Eqs. (1) and (2)) for different polarizations, for the oven-dry wood, with the frequency-independent average dielectric function of cell wall material known, the volume fractions of air and cell wall material can be calculated, and subsequently used to determine the density of a sample.

The calibration procedure used to obtain the dielectric function of cell wall material applied a best-fit procedure to extract the real and imaginary parts separately. The best-fit was defined using the fit for the dielectric function of the cell wall material, combining it with the dielectric function of air, applying the effective medium model, and minimizing the squared difference:

$$Err = \sum_i (\varepsilon_{\text{pred}} - \varepsilon_{\text{meas}})^2 \quad (3)$$

In order to predict the MC of wood materials simultaneously with the density, the dielectric function of water in the wood is necessary. The water can then be incorporated into the measured response by modifying the effective medium theory applied to the oven-dry wood. As water in wet wood is randomly distributed in its cell wall material, the effective medium properties of wet wood can be determined by combining the dielectric function of water and cell wall material. In this way, the prediction of moisture content becomes feasible with the same measurements used to predict density.

In our previous study [15], a double Debye model was used for the dielectric function of water, appropriate for bulk liquid water at frequencies around 1 THz [20]:

$$\varepsilon(\omega) = \frac{\varepsilon_s - \varepsilon_1}{1 - i\omega\tau_1} + \frac{\varepsilon_1 - \varepsilon_\infty}{1 - i\omega\tau_2} + \varepsilon_\infty \quad (4)$$

where the parameters for Eq. (4) were taken as presented in Ref: [20]  $\varepsilon_s = 78.36$ ,  $\varepsilon_1 = 5.16$ ,  $\tau_1 = 7.89$  ps,  $\varepsilon_\infty = 3.49$ , and  $\tau_2 = 0.181$  ps.

As discussed in Section 1, the dielectric function of water will change with moisture content, especially for MCs below the FSP since at a low moisture content, the hydrogen bonding between water molecules and the cellulose and hemicelluloses can be very strong but progresses to much weaker bonding as more water is incorporated into the samples approaching liquid water as the FSP is reached. Therefore, a more accurate model can be expected by taking into account the actual dielectric function of water within the wood rather than the application of the double Debye model used previously, which represents that of bulk liquid water.

To improve the accuracy of the previously reported model, it is expected that the MC-dependent dielectric function of water should be applied. As that functional dependence is currently unknown from a first-principle perspective, a calibration procedure can be implemented similar to what was done for the dielectric function of the cell wall material. In particular, the dielectric function of water at each MC can be fit from measured data for each sample, and subsequently, a MC-dependent effective value can be determined and used consistently within the model.

To incorporate water into the effective medium theory model presented above, the wet wood can be considered to incorporate water, randomly distributed in cell wall material. Such a picture suggests the Bruggeman EMT model is appropriate to incorporate water effects of the hydrated cell wall. Indeed, the Bruggeman model has previously been used to model water within the paper, which is also a cellulose fiber network [21]. The Bruggeman EMT is given by:

$$\varepsilon_{\text{eff}} = \frac{1}{4} \left( \beta + \sqrt{\beta^2 + 8\varepsilon_1\varepsilon_2} \right) \quad (5)$$

$$\beta = (3f_1 - 1)\varepsilon_1 + (3f_2 - 1) \quad (6)$$

In the process of fitting the dielectric function of water, the dielectric function of the wet cell wall material was calculated from the measured values of the dielectric function of the wet wood samples averaged over the frequency range of 0.1–0.2 THz. The dielectric functions of water and cell wall material were combined to determine the dielectric function of the wet cell wall using the Bruggeman EMT model (Eqs. (5) and (6)). The dielectric functions of the dry cell wall material have been determined in the first step as outlined previously, which are  $3.20 + 0.17i$  and  $3.27 + 0.59i$  for parallel and perpendicular polarizations with respect to the THz field, respectively. Therefore, to determine the dielectric function of water, the only parameters required are the volume fractions of each component (cell wall, water, and air) and the model. The volume fractions can be determined independently from physical measurements of density and MC. The best-fit for the dielectric function of water was then determined independently for the real and imaginary parts of the dielectric function by minimizing the difference between the measured dielectric function and predicted by the model using the measured parameters (volume fractions of components from physical measurements).

Finally, the density and moisture content can be determined from a THz measurement as follows. The frequency-independent value obtained for the dielectric function of the cell wall material, combined with the MC-dependent dielectric function of water both obtained as a

calibration, is used in the model to predict the THz response for given volume fractions of air and water ( $f_a$  and  $f_w$ ). The volume fractions are varied, and the difference between the predicted (model) and measured THz response is calculated and minimized to determine the best-fit volume fractions. Those volume fractions correspond to a physical density and moisture content, as explained next.

With the volume fractions  $f_a$  and  $f_w$ , density can be computed using the formula:

$$\rho_{\text{wetwood}} = \rho_a \times f_a + \rho_{\text{ovenw}} \times f_{\text{ovenw}} + \rho_w \times f_w \quad (7)$$

where  $\rho_{\text{wetwood}}$  is the density of wet wood,  $\rho_a$  is the density of air at 20 °C which 0.0012 g cm<sup>-3</sup>,  $\rho_{\text{ovenw}}$  is the average density of the oven-dry cell wall material, which is assumed to be 1.4 g cm<sup>-3</sup> [3],  $\rho_w$  is the density of water which is 1 g cm<sup>-3</sup>, and  $f_{\text{ovenw}}$  is the volume fraction of the oven-dry cell wall material ( $f_{\text{ovenw}} = 1 - (f_a + f_w)$ ).

Similarly, moisture content can be calculated as:

$$\rho_{\text{ovenwood}} = \rho_a \times (f_a + f_w) + \rho_{\text{ovenw}} \times f_{\text{ovenw}} \quad (8)$$

$$\text{MC} = \frac{(\rho_{\text{wetwood}} - \rho_{\text{ovenwood}})}{\rho_{\text{ovenwood}}} \times 100(\%) \quad (9)$$

where the  $\rho_{\text{ovenwood}}$  is the density of the oven-dry wood, and MC is the moisture content of the wood samples.

The reliability of this prediction method can be evaluated by two parameters: the determination coefficient and root-mean-square error (RMSE), defined as follows:

$$R^2 = 1 - \frac{\sum (y - y_{\text{pred}})^2}{\sum (y - \bar{y})^2} \quad (10)$$

$$\text{RMSE} = \sqrt{\frac{\sum (y - y_{\text{pred}})^2}{n - 2}} \quad (11)$$

where  $y$  is the measured value,  $y_{\text{pred}}$  is predicted value that is calculated from the THz measurements,  $\bar{y}$  is the average of the measured value, and  $n$  is the number of samples.

### 3 Results and Discussion

#### 3.1 Simultaneous Prediction of Wood Density and Moisture Content Using the Permittivity of Bulk Water

Here, we summarize previous measurements to which we compare the new results in the section that follows. As explained in Section 2, the prediction of density and moisture content is performed by minimizing the squared difference between the measured and predicted permittivity. The model used in this section relies on the past work where the double Debye



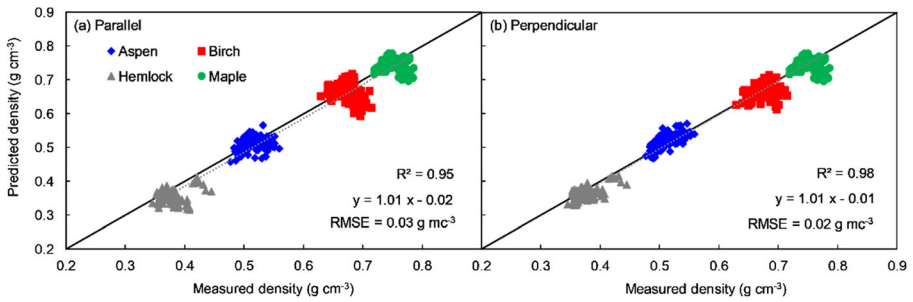


**Fig. 2** Relationship between measured and predicted density based on the previous model.  $R^2$ , determination coefficient; RMSE, root-mean-square error. **a** Parallel and **b** perpendicular refer to the polarization of the THz filed with respect to the grain of the wood samples

model was used for the dielectric function of water, representing that of bulk liquid water. The results are shown in Figs. 2 and 3 for the density and moisture content, respectively.

Figure 2 shows the relationship between the measured and predicted densities, where the important results we need for comparison in the following section are the determination coefficient values  $R^2$  of 0.95 and 0.98 and root-mean-square error (RMSE) values of  $0.03 \text{ g cm}^{-3}$  and  $0.02 \text{ g cm}^{-3}$  for parallel and perpendicular polarizations, respectively. The model provides good prediction at relatively low MCs for both polarizations, and consistently underestimates the real density at higher MCs. The data points that lie furthest from the curve appear at relatively high MC for all species. This can be understood by the fact that wood samples contain more water as the MC increases, which leads to more significant deviations as the improper dielectric function is being used as argued previously. Another contributing factor is the fact that the signal-to-noise ratio is lowest where the sample density and moisture content are the highest.

Figure 3 shows the relationship between measured and predicted MCs, which gives determination coefficient values of  $R^2$  0.88 and 0.75, with root-mean-square error (RMSE) values of 2.53% and 3.34% for parallel and perpendicular polarizations, respectively. The predicted MCs tend to be underestimated at low MC, and gradually approach the measured value as MC increases. This can again be attributed to the behavior of the dielectric function of the water within the wood and is consistent with the summary reported by Inagaki [15]. Specifically, due to the behavior of the dielectric function of water where it is expected that free water absorbs more strongly than bound water, the use of a highly absorbing free water

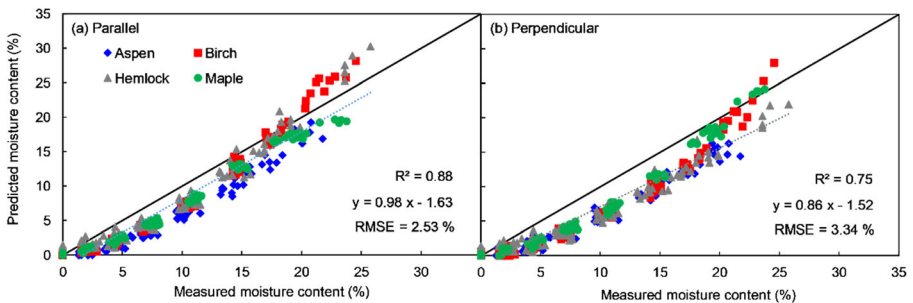


**Fig. 3** Relationship between measured and predicted moisture content based on the previous model.  $R^2$ , determination coefficient; RMSE, root-mean-square error. **a** Parallel and **b** perpendicular refer to the polarization of the THz filed with respect to the grain of the wood samples



dielectric function at low MCs will result in a systematically underestimated value of the MC. Also, as MC increases, the behavior of water molecules progressively approaches that of free water as argued in Section 2, and the predicted MCs will approach the actual values more closely.

### 3.2 Relation Between Dielectric Function and Oven-dry Density and MC

Making measurements of the index of refraction and absorption coefficient for all of the wood samples in the normal way [15], the dielectric function of the wood samples at the various moisture contents was made. Figure 4 shows a clear linear relation and a quadratic relation between moisture content and the real and imaginary parts of the dielectric function for the four species of wood investigated here. The THz beam was polarized perpendicular to the visible grain of the wood samples. A spectral range of 0.1 to 0.2 THz was used, over which individual measurements were averaged to give a single value for the complex dielectric function, in order to approximately satisfy the conditions of validity for the MG-EMT [15].

In a similar fashion, there is a nice relationship between the real and imaginary parts of the measured dielectric functions of the sample and density. The relationship is highlighted in Fig. 5 that shows the measured frequency-resolved real part (a) and imaginary part (b) of the dielectric function that was obtained from THz transmission spectroscopy of oven-dry wood.

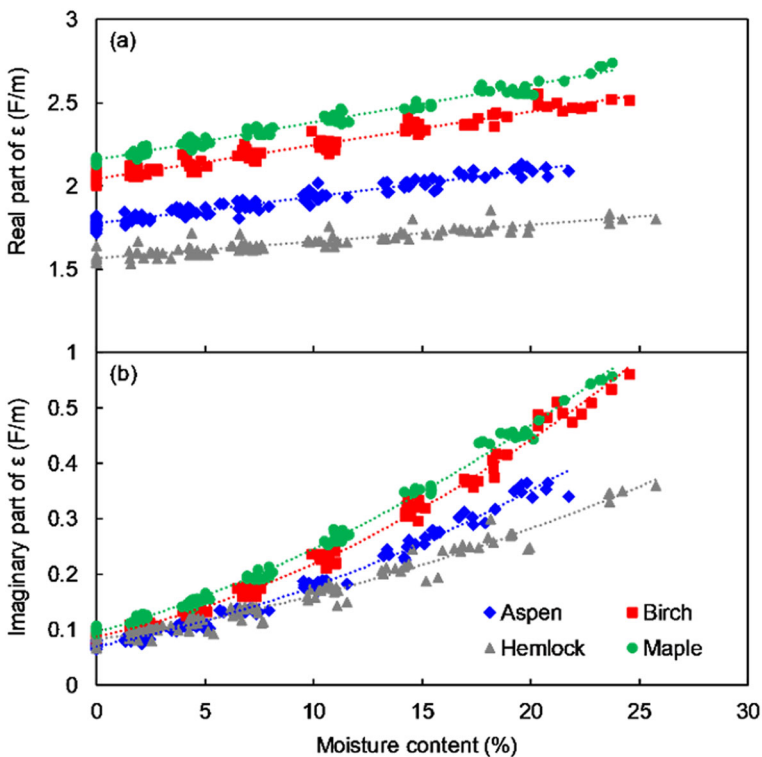


**Fig. 4** Real and imaginary parts of the measured dielectric function for four species of wood as it depends on MC. Measurements are averaged over the frequency range of 0.1–0.2 THz, with the THz beam polarized perpendicular to the grain of the wood samples in the measurements shown

Plots (c) and (d) show the real and imaginary part of the dielectric function averaged over the frequency range of 0.1 to 0.2 THz as a function of MC for birch wood. The THz beam was polarized perpendicular to the visible grain of the wood samples. As shown in Fig. 5, a strong correlation between oven-dry density and the dielectric function is observed that is consistent with other research [22]. The real part of the dielectric function is linear with respect to density, whereas the imaginary part of the dielectric function increases with increasing density. The real and imaginary parts of the dielectric function show a strong correlation with moisture content, as shown in Fig. 6 for birch wood. The real part of dielectric function is relatively linear with respect to MC, whereas the imaginary part of the dielectric function increases quadratically with MC.

The strong correlations between oven-dry density and moisture content and the real and imaginary parts of the measured dielectric function of the wood samples suggest that both density and moisture content can be predicted simultaneously from the THz measurement. Also, it is interesting to note that the real part of the dielectric function increases linearly with MC, while the imaginary part exhibits a quadratic increase, which implies that the imaginary part of the dielectric function of bound water is a function of MC as argued in Section 1.

### 3.3 Calculation of MC-Dependent Dielectric Function of Water

As argued at the start of this report, it is expected that the dielectric function of the water is MC-dependent as it moves from bound to free water through the FSP. It will be shown here that the MC-dependence can be averaged over all species and samples to “calibrate” the measurements with a single MC-dependent dielectric function for the water which will significantly improve the prediction accuracy of the THz measurements. Figure 7 shows the relationship between the volume fraction of water and the best-fit real and imaginary parts of the dielectric function of water averaged over the frequency range of 0.1–0.2 THz. The THz radiation was polarized either parallel or perpendicular to the visible grain of the wood samples. The determination value,  $R^2$ , and significant difference value  $P$  are also showed in

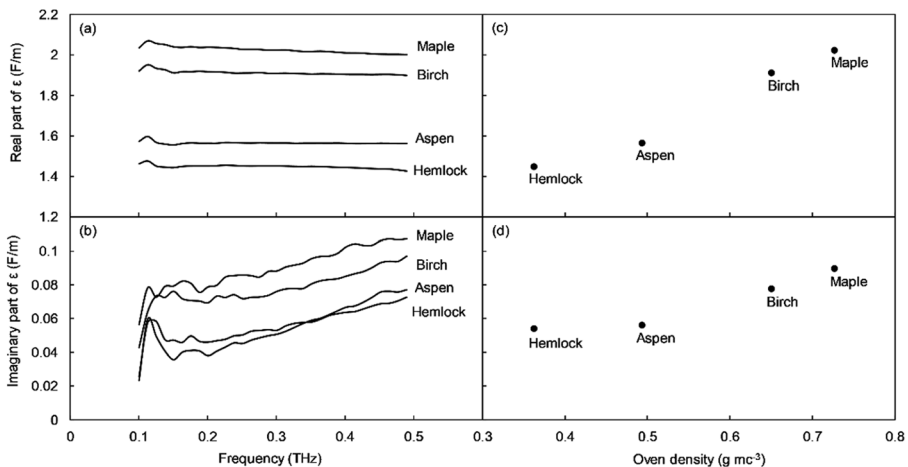


**Fig. 5** Frequency-resolved real part (a) and imaginary part (b) of the measured dielectric function of oven-dry wood samples. Relationship between oven-dry density and the real part (c) and imaginary part (d) of the dielectric function averaged over the frequency range of 0.1–0.2 THz is shown on the right where the THz beam was polarized perpendicular to the grain of the wood samples in these measurements

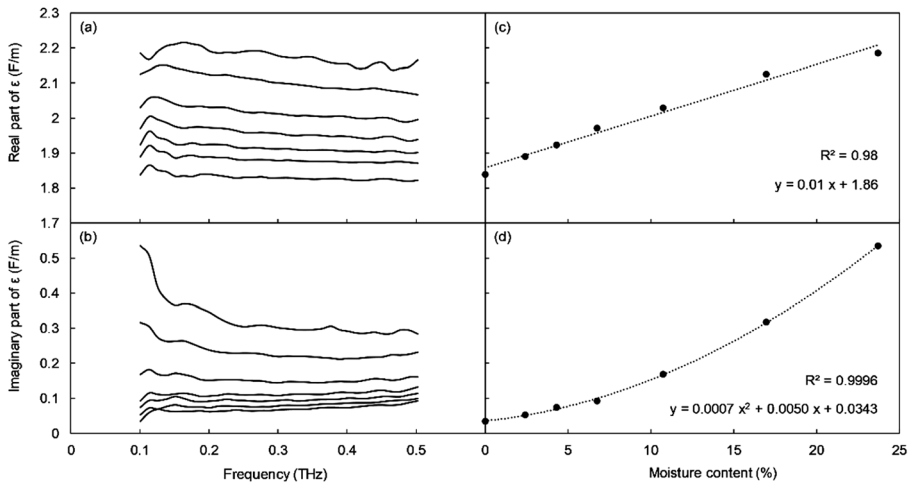


**Fig. 6** Frequency-resolved real part (a) and imaginary part (b) of the measured dielectric function of Birch at various moisture contents. Relationship between moisture content and the real part (c) and imaginary part (d) of the dielectric function averaged over the frequency range of 0.1–0.2 THz the with THz beam polarized perpendicular to the grain of the wood samples

Fig. 7; the real and imaginary parts of dielectric function for both polarizations show extremely small  $P$  values, implying the correlations are reliable.

It can be seen that there is a tendency of the dielectric function to decrease as the volume fraction of water increases for the real part of dielectric function and shows an opposite tendency for the imaginary part of dielectric function. It is worth noting that the dielectric function of water is approximately species independent as reflected by the scatter about the fitting line, can therefore be used for essentially any wood samples just like the dielectric function of cell wall material. Only the volume fraction of water  $> 0.02$  was used here, since

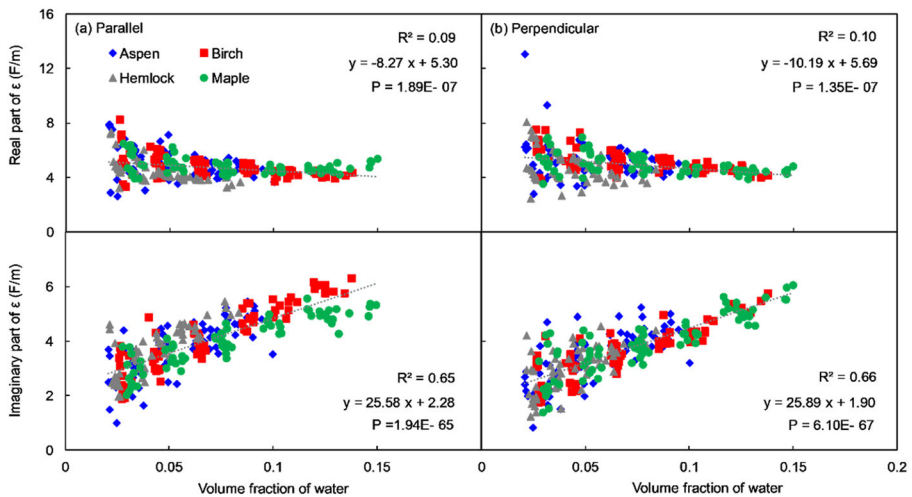


**Fig. 7** Relationship between the volume fraction of water and real and imaginary part of dielectric function averaged over the frequency range of 0.1–0.2 THz.  $R^2$ , determination coefficient;  $P$ , significant difference. a Parallel and b perpendicular refer to the polarization of the THz radiation with respect to grain of the wood samples

using extremely small values for the volume fraction in extracting the dielectric function of water leads to a large error. This is also the reason for the increased spreading of the data with decreasing volume fraction of water as shown in Fig. 7. In particular, hemlock is the only species that appears the dielectric function is not to be spread uniformly about the fitting line, the real part of the dielectric function of water is lower than others and the imaginary part is higher, that suggests the behavior of water probably different from other species.

As outlined in Section 2, the best-fit dielectric function of water was determined based on the dielectric functions of air and cell wall material, with independently determined volume fractions from physical measurements that gave best fits to the experimental data. With the correlation between the best-fit of real and imaginary parts of dielectric function of water and the volume fraction of water, the dielectric function of water can be written as a linear regression for the real and imaginary parts of the dielectric function separately, as a function of the volume fraction of water for the two different polarizations:

$$\epsilon_w^{\parallel} = -8.3 \times f_w + 5.3 + (26 \times f_w + 2.3)i \tag{12}$$

$$\epsilon_w^{\perp} = -10 \times f_w + 5.7 + (26 \times f_w + 1.9)i \tag{13}$$

The principle of the model is also shown in Fig. 8 as described above.

### 3.4 Improvement in Simultaneous Prediction of Wood Density and Moisture Content

With the MC-dependent dielectric function of water now known, the only remaining free parameters are the volume fraction of water and air ( $f_w$  and  $f_a$ ), as the volume fraction of cell wall material is related to these as  $(1 - (f_w + f_a))$ . The model can now be applied, which is a combination of the Bruggeman EMT and MG-EMT models as outlined in Section 2, to extract

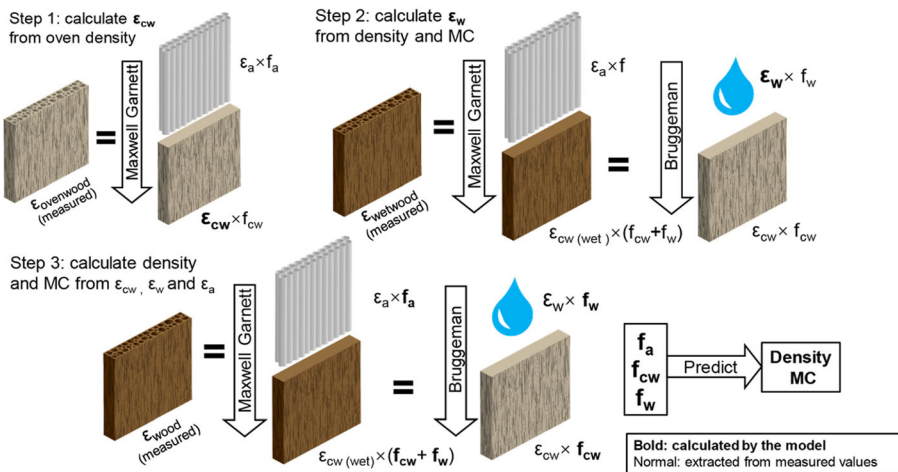


**Fig. 8** Principle of the model. Where  $\epsilon_{cw}$  can be determined by finding the best-fit of the measured dielectric function of oven-dry wood sample, same as the first step, the  $\epsilon_w$  can be determined as a MC-dependent function by finding the best-fit of the measured dielectric function of wet wood sample (discussed in detail in the results). After the calculation of  $\epsilon_{cw}$  and  $\epsilon_w$ , the volume fractions (air, cell wall, water) can be calculated to predict density and MC for wood sample simultaneously

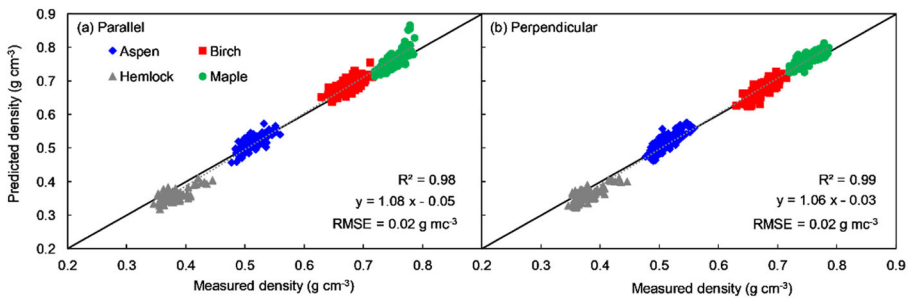


**Fig. 9** Relationship between measured and predicted density based on the new MG-EMT model.  $R^2$ , determination coefficient; RMSE, root-mean-square error. **a** Parallel and **b** perpendicular refer to the polarization of the THz filed with respect to the grain of the wood samples

$f_w$  and  $f_a$ , which gives the predictions for density and MC from the measured THz spectra by using Eqs. (7) and (9).

Figure 9 shows the relationship between the measured and predicted densities using the model with the new MC-dependent dielectric function of water, for both polarization geometries. The new model provides an excellent prediction with a determination coefficient  $R^2$  of 0.98 and 0.99 and RMSE values of  $0.02 \text{ g cm}^{-3}$  and  $0.02 \text{ g cm}^{-3}$ , respectively. This compares favorably with what was previously found in Fig. 2, where the accuracy of prediction has improved compared with the previous one, and the deviation of the predicted values at high MC range has been successfully reduced.

Figure 10 shows the relationship between the measured and predicted MCs by using the MC-dependent dielectric function for water, for both parallel and perpendicular polarizations. A significantly improved correlation between the predicted and measured MCs is observed, with determination coefficient values,  $R^2$ , of 0.92 and 0.95 and RMSE values of 2.22% and 1.69%. Both curves demonstrate improved results in comparison with Fig. 3, and the problem of systematically underestimating of MC has been resolved. It can therefore be concluded that, as has been argued here, the systematic deviation in MC prediction present in Fig. 3 can be attributed to the use of the double Debye model of bulk liquid water for the dielectric function of all water within the wood. Compared with the previous results, the accuracy of prediction has improved by a factor of 2. However, the predictions for hemlock are systematically under-predicted for density and over-predicted for MC, which is certainly related to the deviation of MC-dependent fit of the dielectric function of water as shown in Fig. 7. For hemlock, water

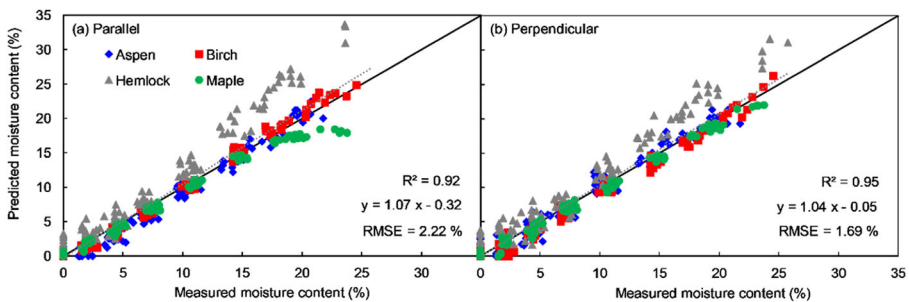


**Fig. 10** Relationship between measured and predicted value of the moisture content based on the use of a MC-dependent dielectric function of water.  $R^2$ , determination coefficient; RMSE, root-mean-square error. **a** Parallel and **b** perpendicular refer to the polarization of the THz filed with respect to the grain of the wood samples

behaving differently from other species, it is probably caused by the different structure and chemical component since hemlock is the only softwood species in our model.

## 4 Conclusions

Terahertz technology is attracting attention in many fields including military radar, biomedicine, and security inspection in recent years. However, THz technology applied to the field of wood quality evaluation is still in its infancy. Previous work has demonstrated the capability for this technology to simultaneously predict density and moisture content below the fiber saturation point in wood. However, the results suffered from systematic errors that were attributed to the use of a dielectric function for bulk water within the wood, when water in wood at low MC undergoes hydrogen bonding within the cellulose network and behaves as bound water. In this report, we demonstrated that the dielectric function of water in wood materials varies with the moisture content of the wood. Further, we showed that the dielectric function of water within the wood is species-independent, and can therefore be calibrated out. This calibration step was performed, and the MC-dependent dielectric function determined. Inserting this function in the model resulted in a significant improvement in the accuracy of the model for both density and moisture content determination and rectified the systematic errors. As a result, we demonstrate a self-consistent model for the simultaneous prediction of density and moisture content.

**Funding Information** This study was financially supported by the Natural Sciences and Engineering Research Council of Canada, Western Economic Diversification Canada, the Northern Development Initiatives Trust, and the JSPS (KAKENHI, No. 16H02559).

## References

1. R. Shmulsky, P. D. Jones, *Forest Products and Wood Science: An Introduction*, 6th ed. (Wiley-Blackwell, West Sussex, 2011), pp. 197–228, 253–288.
2. H. Lilholt, J. M. Lawther, *Comprehensive Composite Materials*. (Elsevier Pergamon Press, Oxford, 2000), pp. 303–325
3. L. Y. Mwaikambo, M. P. Ansell, The determination of porosity and cellulose content of plant fibers by density methods. *J. Mater. Sci. Lett.* 20, 2095–2096 (2001)
4. M. Sovago, R. K. Campen, H. J. Bakker, M. Bonn, Hydrogen bonding strength of interfacial water determined with surface sum-frequency generation. *Chem. Phys. Lett.* 470, 7–12 (2009)
5. C. Skaar, *Wood-Water Relations*. (Springer-Verlag, Berlin, 1988), pp. 1–45, 122–176
6. H. D. Tiemann, Effect of moisture upon the strength and stiffness of wood. (U.S. Dept. of Agriculture, Forest Service, Washington, D. C., 1906), pp 82–84
7. W. T. Simpson, Drying and control of moisture content and dimensional changes, in *Wood handbook: wood as an engineering material*, (USDA Forest Service, Forest Products Laboratory, General technical report FPL; GTR-113; Madison, WI, 1999), p 12.1–12.20.
8. J. B. Jackson, M. Mourou, J. Labaune, J. F. Whitaker, I. N. Duling III, S. L. Williamson, C. Lavier, M. Menu and G. A. Mourou, Terahertz pulse imaging for tree-ring analysis: a preliminary study for dendrochronology applications. *Meas. Sci. Technol.* 20, 075502 (2009)
9. M. Koch, S. Hunsche, P. Schumacher, M. C. Nuss, J. Feldmann and J. Fromm, THz-imaging: a new method for density mapping of wood. *Wood Sci. Technol.* 32, 421–427 (1998)
10. Y. Wang, S. She, N. Zhou, J. Zhang, H. Yan and W. Li, Wood Species Identification Using Terahertz Time-domain Spectroscopy. *BioResources* 14, 1033–1048 (2018)
11. M. Bensalem, A. Sommer, J. C. Mindeguia, J. C. Batsale and C. Pradere, Terahertz Measurement of the Water Content Distribution in Wood Materials. *J. Infrared, Millimeter, Terahertz Waves* 39, 195–209 (2018)

12. M. Scheller, S. Wietzke, C. Jansen and M. Koch, Modelling heterogeneous dielectric mixtures in the terahertz regime: a quasi-static effective medium theory. *J. Phys. D: Appl. Phys.*, 42(6): 065415 (2009)
13. C. Jördens, S. Wietzke, M. Scheller and M. Koch, Investigation of the water absorption in polyamide and wood plastic composite by terahertz time-domain spectroscopy. *Polym. Test.*, 29(2): 209–215 (2010)
14. T. Inagaki, I. D. Hartley, S. Tsuchikawa and M. Reid, Prediction of oven-dry density of wood by time-domain terahertz spectroscopy. *Holzforschung* 68, 61–68 (2014)
15. T. Inagaki, B. Ahmed, I. D. Hartley, S. Tsuchikawa and M. Reid, Simultaneous prediction of density and moisture content of wood by terahertz time domain spectroscopy. *J. Infrared, Millimeter, Terahertz Waves* 35, 949–961 (2014)
16. Y. Oyama, L. Zhen, T. Tanabe and M. Kagaya, Sub-terahertz imaging of defects in building blocks. *NDT&E Int.* 42, 28–33 (2009)
17. L. Duvillaret, F. Garet, J. L. Coutaz, A reliable method for extraction of material parameters in terahertz time-domain spectroscopy. *IEEE J. Sel. Top. Quantum Electron.* 2, 739–746 (1996)
18. M. Reid, R. Fedosejevs, Terahertz birefringence and attenuation properties of wood and paper. *Appl. Opt.* 45, 2766–2772 (2006)
19. Z. Hashin, Analysis of composite materials—a survey. *J. Appl. Mech.* 50, 481–505 (1983)
20. P. U. Jepsen, U. Möller, H. Merbold, Investigation of aqueous alcohol and sugar solutions with reflection terahertz time-domain spectroscopy. *Opt. Express* 15, 14717–14737 (2007)
21. P. Mousavi, F. Haran, D. Jez, F. Santosa and J. S. Dodge, Simultaneous composition and thickness measurement of paper using terahertz time-domain spectroscopy. *Appl. Opt.* 48, 6541–6546 (2009)
22. S. Tanaka, K. Shiraga, Y. Ogawa, Y. Fujii and S. Okumura, Applicability of effective medium theory to wood density measurements using terahertz time-domain spectroscopy. *J. Wood Sci.* 60, 111–116. (2014)

**Publisher's Note** Springer Nature remains neutral with regard to jurisdictional claims in published maps and institutional affiliations.